0270-6474/83/0308-1554$02.00/0

The Journal of Neuroscience
Vol. 3, No. 8, pp. 1554-1564
August 1983

AN ANALYSIS OF AXON CALIBER WITHIN THE OPTIC NERVE OF THE CAT: EVIDENCE OF SIZE GROUPINGS AND REGIONAL ORGANIZATION[1]

ROBERT W. WILLIAMS[2] AND LEO M. CHALUPA[3]

Department of Psychology and the Physiology Graduate Group, University of California, Davis, California 95616

Received December 2, 1982; Revised March 3, 1983; Accepted March 4, 1983

Abstract

Axon size in the optic nerves of three adult cats was measured using an accurate planimetric method. A sample of the axon complement was obtained from sets of more than 125 electron micrographs taken of each nerve. In contrast to previous reports, the distribution of axon diameter, as estimated from measurements of axonal cross-sectional area, was clearly bimodal. The group of finest axons had a mode at approximately 1 μm, and the mode of the group of intermediate size axons was approximately 2 μm. Fibers with diameters larger than 3.5 μm formed the extensive tail of the distribution. The proportions of large, intermediate, and small axons were estimated to be 5%, 45%, and 50%. These groups probably correspond to the α, β, and γ classes of retinal ganglion cells. Regional distributions of axon caliber were also bimodal and, in a few instances, even trimodal. A peripheral crescent of each nerve contained a large number of fine fibers. Mean fiber diameter within discrete regions of the optic nerve varied inversely with the density of axon packing. The thickness of the myelin sheath was highly correlated with the inner fiber diameter; hence, myelin sheath width was also distributed in a bimodal manner. These results furnish the first clear evidence that the distribution of fiber caliber within the cat's optic nerve mirrors the principal classes of retinal ganglion cells.

Visual information from the retina of the cat is transmitted via discrete channels. This was initially suggested by the discovery of distinct components in field potentials recorded from the optic nerve and tract (P. O. Bishop et al., 1953; G. H. Bishop and Clare, 1955; Chang, 1956; G. H. Bishop et al., 1969). Subsequent studies have defined three functional classes of retinal ganglion cells, termed X, Y (Enroth-Cugell and Robson, 1966), and W (Stone and Hoffmann, 1972), a categorization which is based on receptive field properties and conduction velocity (Cleland et al., 1971; Hoffmann, 1973; Stone and Fukuda, 1974). Complementary anatomical studies of the cat's retina have also described three principal classes of ganglion cells, α, β, and γ, which are distinguished by the disposition of dendrites and the size of the cell body (Boycott and Wässle; 1974; Kelly and Gilbert, 1975; Peichl and Wässle, 1979; Wässle and Illing, 1980; Illing and Wässle, 1981; Wässle et al., 1981). There are compelling reasons to believe that α, β, and γ cells correspond to Y, X, and W functional types (for review see Lennie, 1980).

Virtually all fibers within the adult cat's optic nerve are myelinated (Hughes and Wässle, 1976; Stone and Campion, 1978; Williams et al., 1983). With few exceptions, the conduction velocity of myelinated fibers varies directly with fiber diameter (Gasser and Grundfest, 1939; Rushton, 1951; Ogden and Miller, 1966; Waxman and Swadlow, 1977; Cullheim and Ulfhake, 1979). Given the tripartite division of the conduction velocity of retinal ganglion cells (e.g., Rowe and Stone, 1976), it might be anticipated that the caliber of axons in the cat's optic nerve would be distributed in a trimodal manner. Surprisingly, however, studies which have examined this problem have found the cumulative distributions of fiber diameter to be unimodal (G. H. Bishop and Clare, 1955; G. H. Bishop et al., 1969; Donovan, 1967; Friede et al., 1971; Hughes and Wässle, 1976; Freeman, 1978). Although several explanations have been put forward to explain this apparent paradox (G. H. Bishop and Clare, 1955; Stone and Holländer, 1971; Cleland et al., 1973; Freeman, 1978), these are not entirely satisfactory. Therefore, we have re-examined, in detail, the size distribution of axons in the cat's optic nerve.

[1] The authors wish to acknowledge the essential and expert assistance of Dr. Michael J. Bastiani. This work was supported by Grant EYO-3991 from the National Eye Institute to L. M. C. and a Jastro-Shields Research Award to R. W. W.

[2] Present address: Section of Neuroanatomy, Yale University School of Medicine, 333 Cedar Street, New Haven, CT 06510.

[3] To whom correspondence should be addressed.

Materials and Methods

Optic nerves were taken from three normal adult cats. The animals were deeply anesthetized with sodium pentobarbital and perfused with heparinized saline followed by 2.5% glutaraldehyde/2.5% paraformaldehyde in 0.1 M phosphate buffer, pH 7.3. Within the next 12 hr the optic nerves, chiasm, and tracts were dissected free as one X-shaped piece. The dural sheath was removed, and several 1-mm thick pieces of the nerve were cut by hand as closely as possible to a transverse plane at a site midway between the eye and the chiasm, approximately 6 to 8 mm distal to the chiasmic junction. The particular level of the nerve chosen for analysis appears to have no appreciable effect upon the overall distribution of axon diameter (R. W. Williams and L. M. Chalupa, unpublished data). The final adjustment of the cutting plane was made prior to ultramicrotomy. Tissue processing for electron micrography was identical to that detailed in a previous paper (Williams et al., 1983). As judged by the appearance of the myelin lamellae and the microtubules, the large majority of fibers were sectioned close to the normal plane. Furthermore, it should be noted that the measurement method is, within wide limits, minimally affected by fibers cut at an angle: for instance, obliquity as great as 30° results in only an 8% overestimate of fiber diameter.

Analysis. Photographs of complete ultrathin sections through each of the nerves were taken with a Hitachi HU-11E electron microscope. The image magnification was × 2300, and the final magnification on the prints used for quantification ranged from × 5100 to 5600. The precise magnification was determined with the aid of a calibration grid. Micrographs were taken with strict reference to the grid bars even if large glial processes or blood vessels happened to be included in the field. Furthermore, the sample fields were dispersed evenly across the entire face of the section. Hence, the pool of micrographs represents each region of the nerve in proportion to its contribution to the total section area.

Quantification of axon dimensions was made with the aid of a computer and digitizing tablet (Zeiss Videoplan). The measuring resolution of this system is 0.2 to 0.3 mm, which at a print magnification of × 5000 gives a maximum resolution of 0.05 μm. The area and perimeter of the axon proper, excluding the myelin sheath, were the primary measurements. Axon diameter was derived from the area measurement; thus, this measure actually represents the diameter of a circle with an area equal to that of the axon. The accuracy of individual measurements, tested by repeated calculations of axon diameter, was typically ± 5%.

The relation between inner axon diameter and myelin sheath thickness was assessed in two ways. Initially we projected an image of individual axons onto the digitizing tablet at a magnification of × 24,000. This provided sufficient resolution to determine the myelin sheath width, and 500 axons were measured in this way. In an additional 471 fibers the internal and external areas were measured separately and were converted to equivalent radii; the difference between these measurements provided an estimate of the sheath width. Both procedures yielded essentially the same results.

Results

The numbers of axons within the three nerve sections were estimated to be 159,000 ± 3,400, 158,000 ± 4,000, and 164,000 ± 4,100. The methodology employed to assess the total axon complement has been described previously by Williams et al. (1983). Estimates of the total axon number and the regional fiber packing density of AC1 and AC2 were reported in that study. The present analyses of axon caliber are based on 129 micrographs (covering 8.6% of the section area) in AC1, 139 micrographs in AC2 (8.4%), and 150 in AC3 (10.1%).

Figure 1 shows the cumulative distribution of axon diameter for the three nerve sections, and, as may be seen, the diameter spectra are clearly bimodal. The finest fibers form a prominent peak centered between 0.8 and 0.9 μm. The second contingent, composed of intermediate caliber axons, has a broader distribution with a mode between 1.8 and 2.3 μm. In each histogram a prolonged

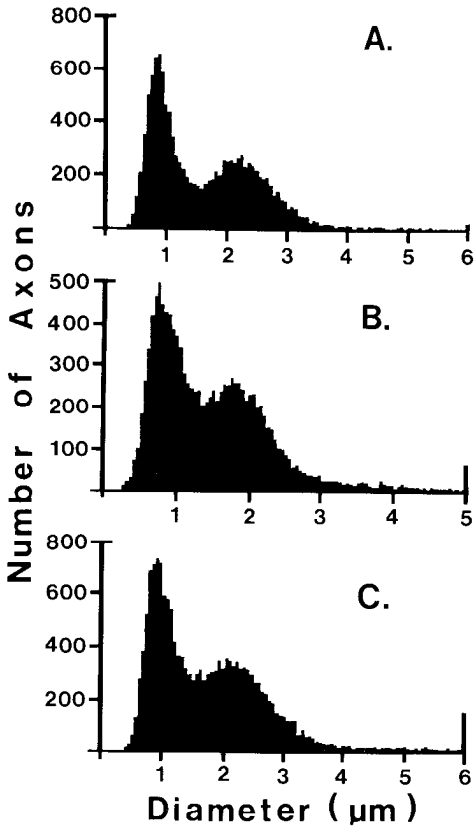

Figure 1. Cumulative distributions of inner axon diameter in the optic nerve. Histograms are composed of 100 bins and were constructed using the Zeiss Videoplan system. The *ordinate* in these and all subsequent histograms gives the absolute frequency. *A*, The distribution from AC1; a bimodal spectrum with modes at 0.87 and 2.25 μm is readily apparent. The histogram is based on the measurement of 12,578 axons. The tail of the distribution extends from 3.5 to 6.0 μm. Thirty-two fibers had a diameter greater than 6 μm, and these have been collected in the last bin of the histogram. Mean fiber diameter is 1.69 μm. *B*, The distribution of 11,936 fibers from AC2; the modes occur at 0.81 and 1.77 μm. Fifty-eight fibers had diameters greater than 5 μm. The average fiber diameter in this specimen is 1.48 μm. *C*, The distribution of 16,477 fibers from AC3 with modes at 0.93 and 2.07 μm. The mean diameter is 1.78 μm.

tail consisting of the largest fibers extends beyond 3.5 μm. A few fibers had diameters between 6.0 and 8.0 μm, and these are shown to the far right of the histograms. There is some variability in the relative size and separation of the peaks. The factors underlying these differences are unknown, but could include: (*i*) natural variation, (*ii*) differences in tissue fixation and processing, or (*iii*) the particular location of the nerve section.

The bimodal distribution can be recognized occasionally in individual micrographs. A complete sample field taken from the bottom sector of AC3 is reproduced in Figure 2. The intermediate size fibers dominate the field. However, a large number of fine and inconspicuous axons are interspersed in the interstices between larger fibers, particularly within the upper half the micrograph.

A systematic analysis of fiber size restricted to discrete regions within each nerve cross-section was carried out to determine the relation between global and local properties of the fiber size spectrum. This problem is of considerable interest, since it is known that there is a striking regional segregation according to fiber size in the cat's optic tract (e.g., Guillery et al., 1982). The results of our analysis are shown in Figures 3 through 6. Individual histograms were derived from sets of micrographs taken from particular sectors of the nerve face. For example, in the case of AC1 the 129 micrographs were divided into 13 sets, each originating from the region on which the histogram has been placed upon the outline of the nerve. Figure 3 shows the distribution of axon perimeter, and Figure 4 that of diameter for this

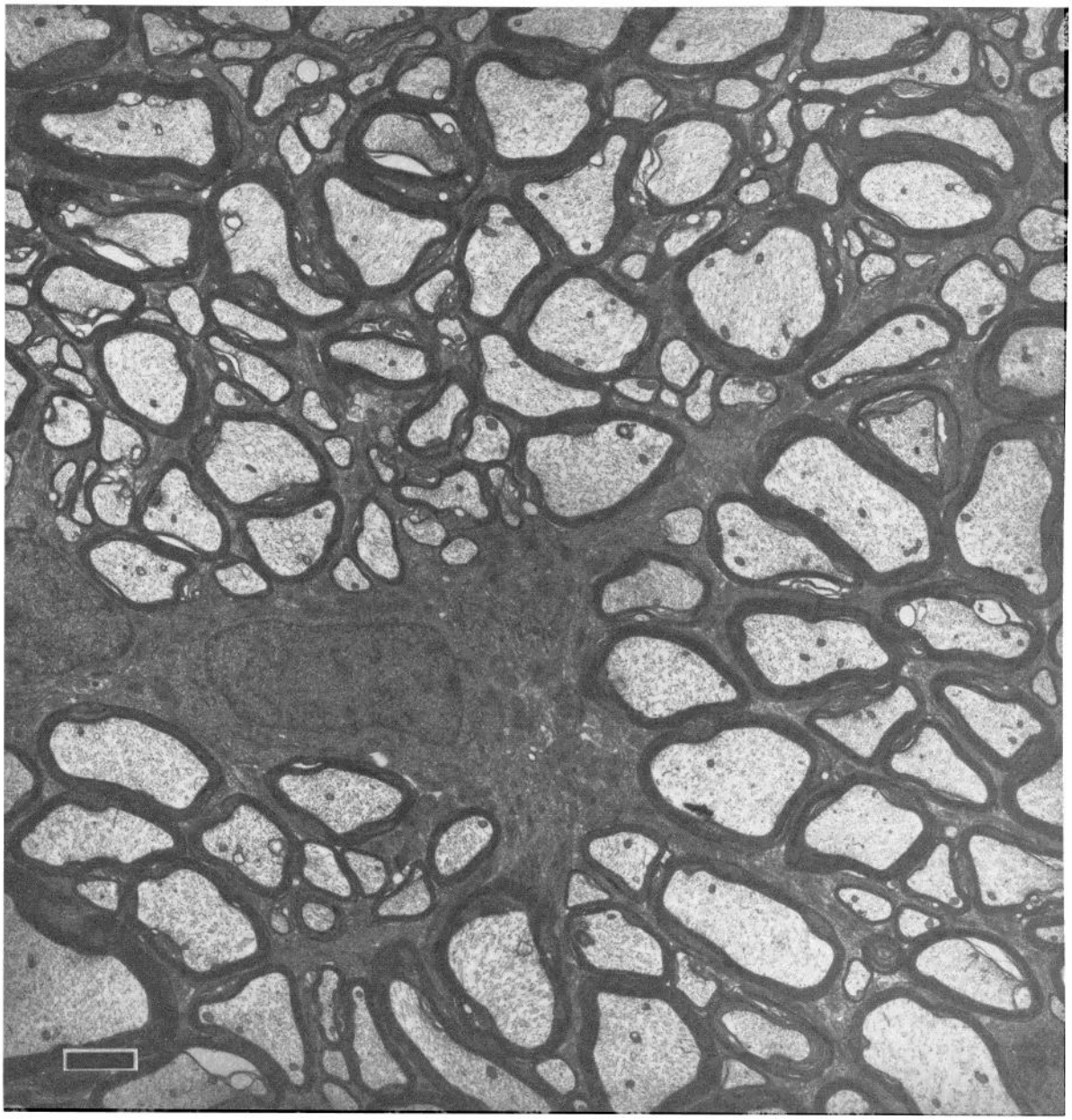

Figure 2. One of 150 sampling micrographs taken from the optic nerve of AC3. The position of the 1,200 μm^2 field covered by this micrograph is marked by a *small arrow* in Figure 7. A division of axons into two size groups can be discerned. Axon profiles are not, in general, circular. *Calibration bar* represents 2 μm.

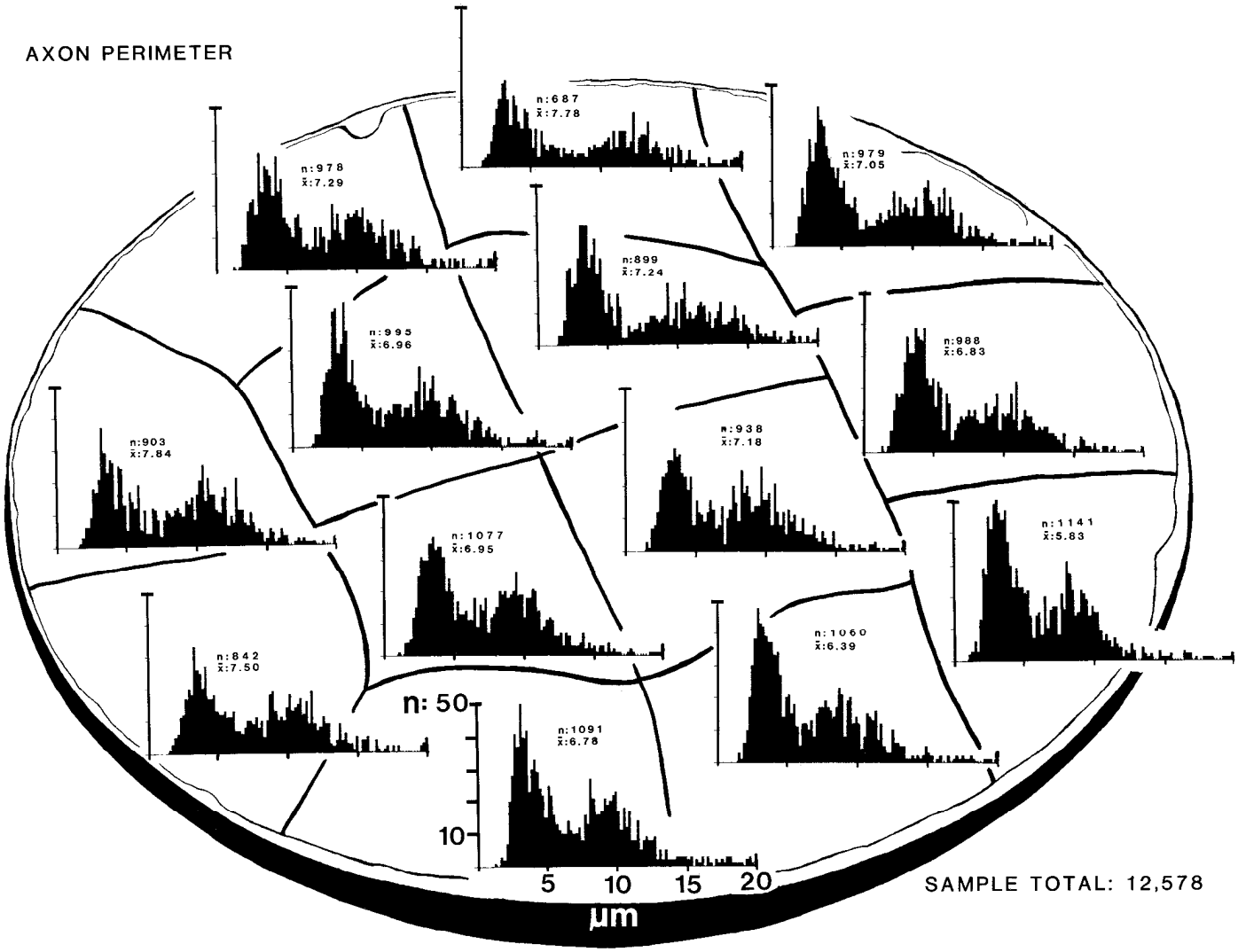

Figure 3. Regional distribution of inner axon perimeter from AC1. Thirteen histograms based on measurements taken from groups of 8 to 11 neighboring micrographs are shown superimposed on a schematic outline of the nerve section. The number of axons and their mean perimeter are shown above the histograms. The first mode of these distributions averages 3.0 μm; that of the second averages 10.0 μm. Histograms to the right correspond to the peripheral crescent of the nerve which contains large numbers of finer axons (see the text). The orientation of the nerve section was not preserved during histological processing. However, based upon the work of Guillery (1970), we can deduce their approximate orientation. For this and all subsequent figures of nerve sections, lateral (temporal) is to the right, and the dorsal sector of the nerve is up.

animal. Similar analyses were carried out for AC2 and AC3. Because the perimeter and diameter measurements yielded essentially the same result, only the latter are depicted in Figures 5 and 6.

As in the case of the cumulative distributions, there is considerable variability between animals in the shape of the regional histograms. Nevertheless, bimodal distributions are evident in each histogram from AC1 (Fig. 4) and AC3 (Fig. 6), and in all but four from AC2 (Fig. 5). In some sectors a break in the distribution can be seen at the base of the second curve. Beyond this break a small number of large axons (approximately 5%) contributes to an extensive and relatively flat tail. However, more commonly the intermediate portion of the distribution tapers gradually into the long tail without any clear discontinuity.

In each nerve there is a rough gradient of average fiber size across the nerve face. Sectors to the right in each figure have the lowest means, whereas diametrically opposed regions have the highest means. In the case of AC1 the average shifts from a minimum of 1.44 to 1.91 μm, in AC2 from 1.31 to 1.80 μm, and in AC3 from 1.60 to 1.89 μm. A careful inspection of the figures reveals that the shift toward higher mean axon diameter is due to two factors: (*i*) a decrease in the number of the smallest fibers and (*ii*) a displacement of the mode of the medium caliber axons toward larger values.

We have previously shown (Williams et al., 1983) that axon packing density within the cat's optic nerve is not uniform at midorbital sites. Specifically, in each of the three nerves a peripheral crescent was characterized by very high packing density. This is shown graphically in Figure 7 for AC3. Equivalent data for the other two animals have been presented in Williams et al. (1983).

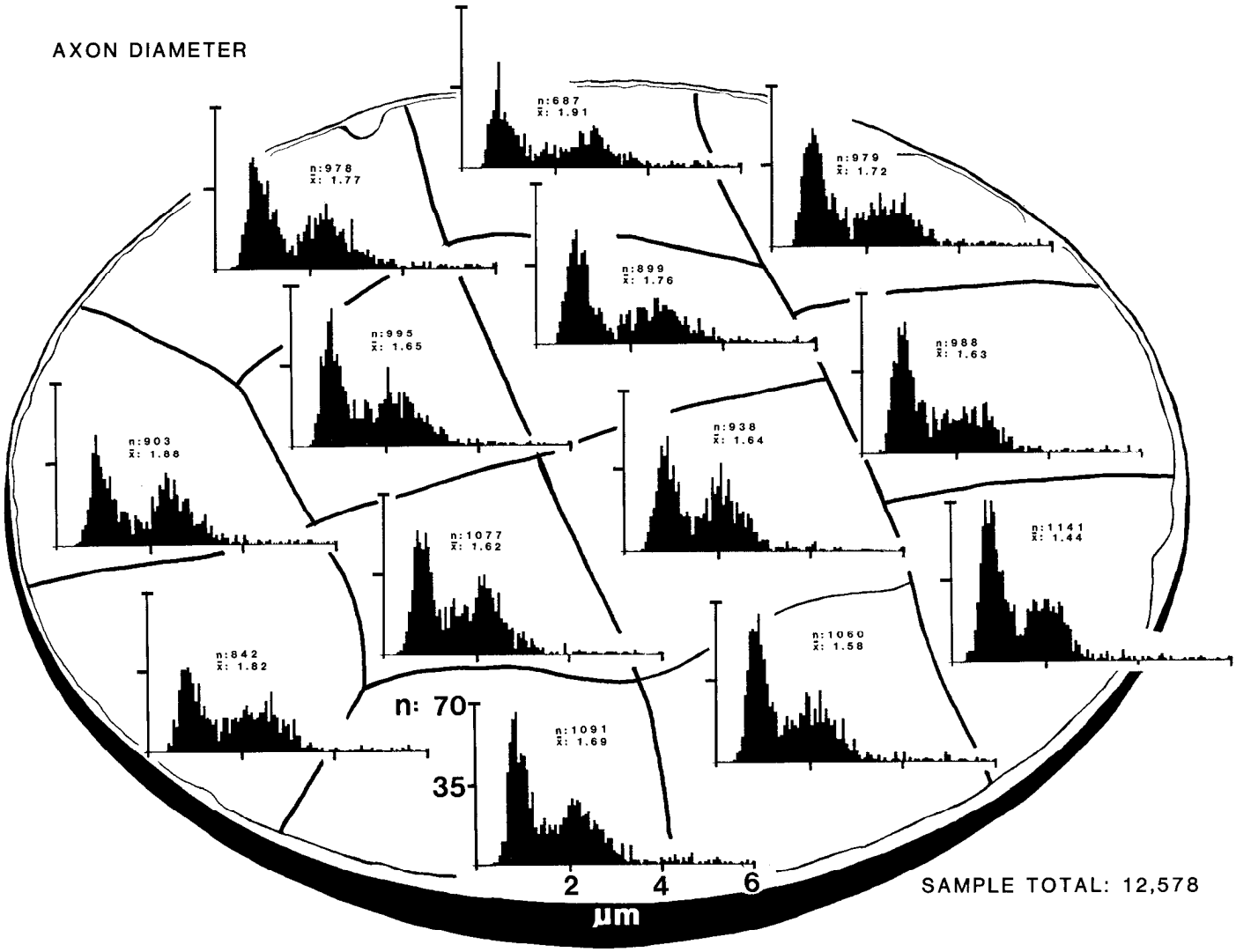

Figure 4. Regional distribution of inner axon diameter for AC1. This figure is arranged in a fashion similar to Figure 3. The mode of the small axon complement is approximately 0.9 μm, whereas that of the intermediate group ranges from 1.9 to 3.0 μm. Note that within the peripheral crescent of the section, shown to the right of the figure, there is a relative abundance of fine fibers, as well as a shift of the intermediate group toward a lower mean caliber.

The work of Guillery provides a means to identify this region of high axon density as the lateral margin of the nerve (Guillery, 1970, p. 355). By comparing the histograms in Figure 6 with Figure 7, it can be seen that axon size and packing density are related inversely. Thus, the lateral crescent of the nerve which contains the largest number of axons has a distribution skewed toward smaller sizes. A similar region of high axon density is also discernible in the light microscopic analysis of the cat's optic nerve provided by Donovan (1967). Since the distribution of glia and blood vessels within the nerve parenchyma is quite uniform at the midorbital level, the gradient in packing density is not secondary to a regional variation in the distribution of these elements.

We have estimated the proportion of the small and intermediate fiber complement contributing to the cumulative sample by bisecting the individual sector histograms at the location of the trough between the small and intermediate groupings. The same procedure was also applied to the cumulative histograms. On the basis of this analysis we estimate that 48 to 52% of the axon population comprise the small axon elevation of the histogram, while between 43 and 47% of the axons are of intermediate size. The tail of the distribution, made up of axons thicker than 3.5 μm, contributes the remaining 4 to 6% of the population. These proportions are virtually identical to those estimated by Rodieck (1973) using the data of G. H. Bishop et al. (1969). In contrast, however, the proportion of β cells has been estimated to be 53 to 57% (Illing and Wässle, 1981), roughly 10% more than our estimate of the proportion of intermediate size axons. Conversely, estimates of the γ cell complement range from 38 to 41% (Illing and Wässle, 1981), whereas our estimate of the small axon component is 48 to 52%. Given the differences in the methodology underlying the tripartite division of retinal ganglion cells and their axons, the significance of these discrepancies is obscure. Experiments considered in the "Discussion"

could resolve this problem, and allow a complete dissection of the region of overlap between small and intermediate size fiber groups.

Myelin thickness. Figure 8 shows the distribution of myelin thickness for 500 axons taken from the bottom sector of AC1. As was the case for inner fiber diameter, the distribution of myelin thickness is clearly bimodal. The suggestion that myelin sheath width is correlated with inner fiber diameter is confirmed by the scatter diagram in Figure 9. The correlation between inner and outer diameter is highly significant ($r = 0.995$). Goldman and Albus (1968) have calculated that the optimal ratio of internal to external diameter for attaining effective internodal current spread (termed the g value) should range between 0.60 and 0.75 (also see Jack et al., 1975, for review). The g value we have calculated, defined as the slope of the regression line, is 0.80. Thus, the myelin sheath thickness is on average one-fourth that of the internal axon radius; for instance, an axon with a 2.0-μm diameter will have an external diameter of 2.5 μm.

An unanticipated outcome of plotting the inner-outer fiber diameter data was the clear division obtained between intermediate and large caliber axons. In the scatter diagram shown in Figure 9, fibers with an outer fiber diameter above 4 μm emerge as a dispersed, but nonetheless distinct, group ($n = 23$), and these comprise 5% of the sample.

Discussion

These findings resolve a long-standing conflict between morphological and physiological observations on the cat's optic nerve. Morphological results on the distribution of axon caliber in the nerve now concur with conduction velocity data obtained from the population of retinal ganglion cells. Axon caliber in the cat's optic nerve is distributed in a bimodal manner. The smallest class of axons, with diameters ranging from 0.3 to 1.5 μm, makes up 48 to 52% of the population, and the intermediate caliber class, between 1.5 and 3.5 μm in size, comprises 43 to 47%. A third group of exceptionally large axons, with diameters between 3.6 and 8.0 μm, forms the prominent tail of the diameter distribution, and these account for the remaining 4 to 6% of the population.

The subdivisions of the size spectrum most likely correspond to the principal classes of retinal ganglion

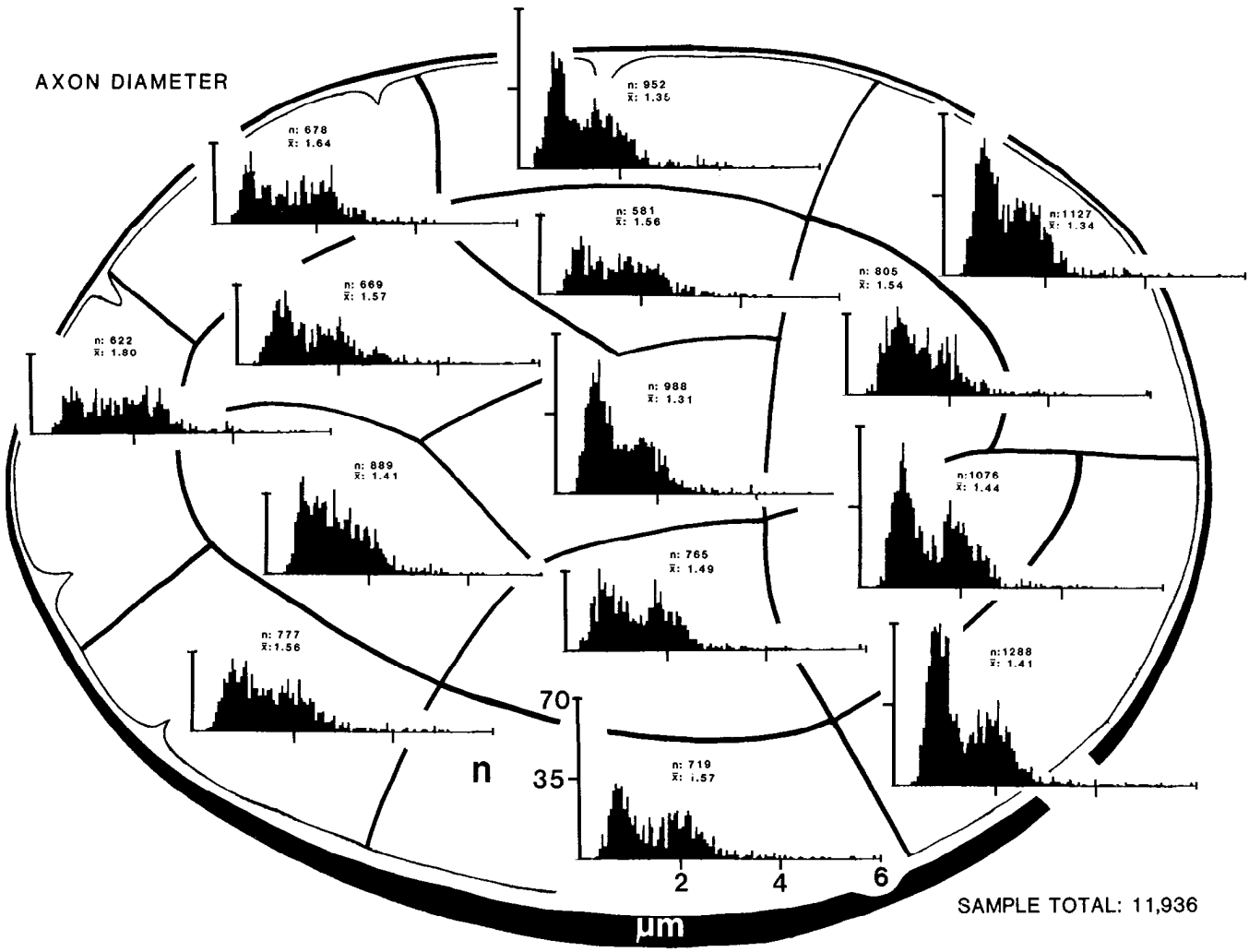

Figure 5. Regional distribution of axon diameter in AC2. Conventions are as in Figures 2 and 3. The first mode is approximately 0.79 μm. The second mode is poorly defined but appears to range between 1.8 and 2.5 μm.

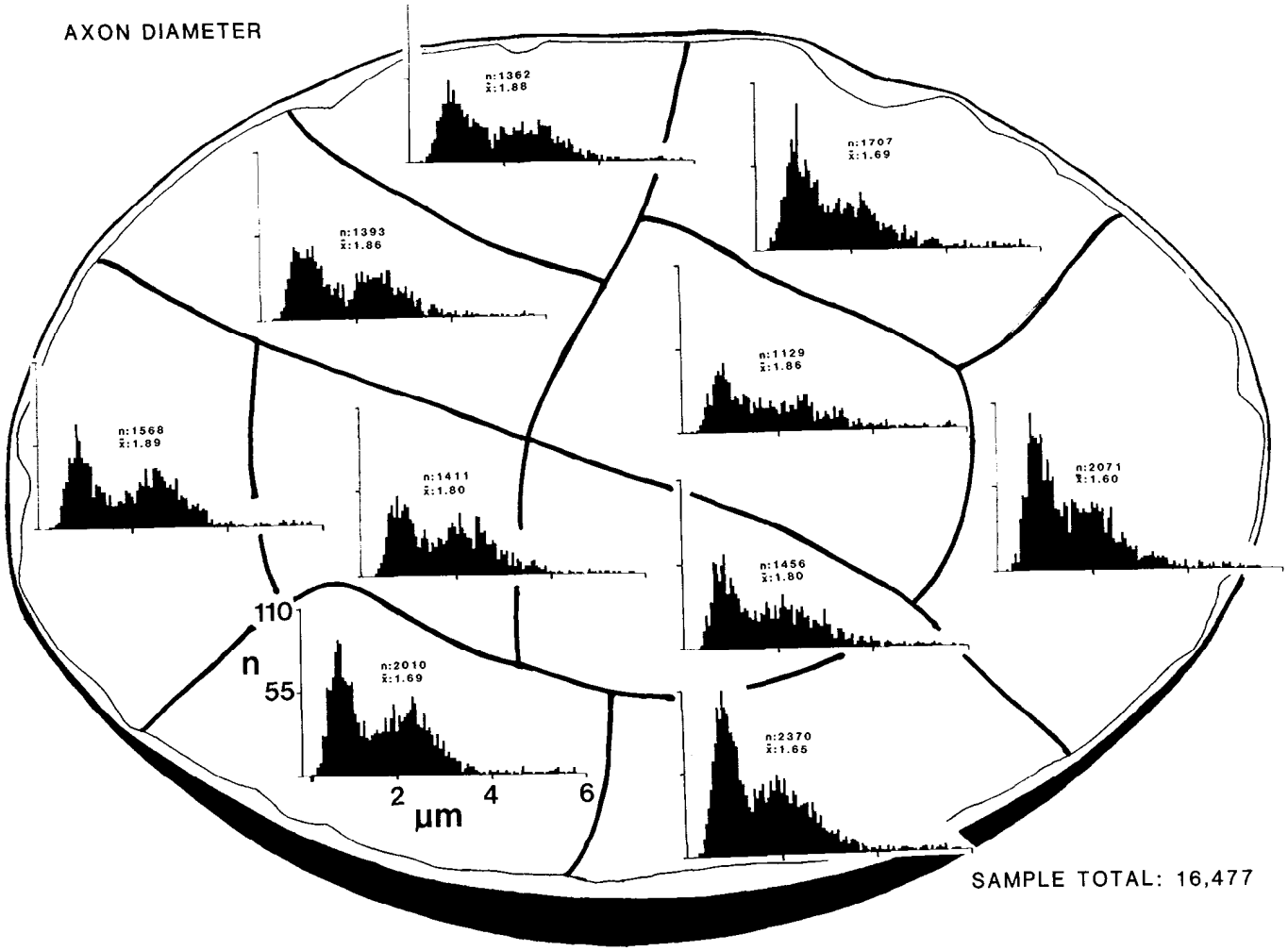

Figure 6. Regional distribution of axon diameter in AC3. Conventions are as in Figures 2 and 3. The first mode is approximately 0.9 μm. The second mode is between 1.9 and 2.8 μm.

cells established by previous physiological and morphological studies cited in the introduction. The majority of the small diameter group probably originate from the somata of the γ cell class.[4] The intermediate group are likely to stem from the β cells, and the largest fibers from the α neurons. Given this scheme one would predict that the distribution of ganglion cell soma size would mirror that of fibers within the nerve. A bimodal spectrum of somal area, almost indistinguishable from many of our regional histograms, has, in fact, been presented by Peichl and Wässle (1979, Fig. 8).

If the foregoing interpretation is correct, it may be asked why a third mode was not apparent in the cumulative histograms of Figure 1. The absence of a third mode might, however, be expected because of the relative paucity of very large neurons (between 4 and 6%) and the comparatively dispersed distribution of their perikaryal size (see Fig. 9 of Boycott and Wässle, 1974; Fig. 8 of Peichl and Wässle, 1979; and Fig. 13*A* of Wässle and Illing, 1980). It should be noted that, although axons with diameters above 3.5 μm are a minor numerical constituent, they occupy a substantial portion of the nerve. The largest 5% of the axon complement accounts for between 20 and 25% of the summed area of all axon profiles. In comparison, the smallest 45% of the fiber population occupies a mere 10 to 12% of this area.

The identity between fiber groups described in this section and the classes of retinal ganglion cells which give rise to them could be established in several ways. Injections of peroxidase into the superior colliculus label preferentially the γ and α ganglion cells (Kelly and Gilbert, 1975; Magalhães-Castro et al., 1976; Wässle and Illing, 1980). Electron microscopic histochemistry on the nerve should demonstrate label within the small and very large axon contingents. Conversely, injections restricted to laminae A and A1 of the lateral geniculate nucleus should label selectively the intermediate and large fiber groups. Another approach would take advantage of the recent innovation of Spear and his colleagues (Spear et al., 1982; Kornguth et al., 1982), who have been able to eliminate a substantial proportion of the largest ganglion cells by intravitreal injections of antibodies. The appli-

[4] Ganglion cells of the cat retina can be subdivided into additional categories on the basis of somal and dendritic cytological characteristics (e.g., Boycott and Wässle, 1974; Leventhal et al., 1980; Stone and Clarke, 1980). However, a substantial majority of ganglion cells are adequately subsumed within the tripartite division described above.

cation of these antibodies should also decrease the number of very coarse axons, as well as the cross-sectional area of the nerve.

The small, intermediate, and large fiber classes were found in all sectors of the optic nerve. In contrast, fibers of different sizes are more neatly parceled in the optic tract; the thickest fibers are restricted to the ventral sector, the intermediate fibers are situated in the dorsomedial part of the tract, and the finer fibers are scattered through most of the tract but are especially concentrated ventrolaterally (Chang, 1956; P. O. Bishop et al., 1953; G. H. Bishop and Clare, 1955; Guillery et al., 1982). It has been suggested that this foreshadows the separation of functional types within the laminae of the dorsal lateral geniculate nucleus (Guillery et al., 1982). The regional variation of axon size within the nerve is more subtle and is correlated with the numerical density of axon bundles. The difference in the degree of segregation of fibers by size in the nerve and tract can be appreciated by comparing Figures 4 to 6 with Figure 3 from Guillery et al. (1982).

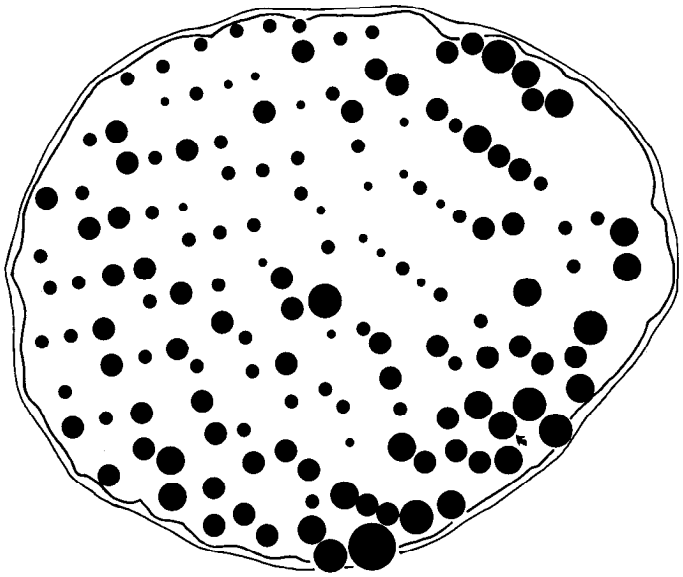

Figure 7. Map of axon packing density for AC3. Each spot represents an individual sampling micrograph, such as shown in Figure 2. The size of the spot indicates the approximate number of axons counted in a field of 1,200 μm^2. The spot marked by the *arrow* indicates the position of the micrograph shown in Figure 2. Similar maps for AC1 and AC2 have been presented in Figure 8 of Williams et al. (1983). The lateral portion of the nerve is to the right, and the dorsal portion is uppermost.

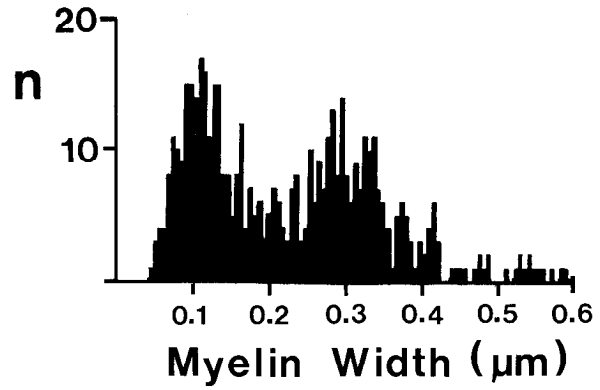

Figure 8. Distribution of myelin sheath thickness. The sample of 500 fibers originated from the bottom left sector of AC1. The histogram of myelin sheath width mirrors that of fiber diameter with modes at 0.12 and 0.29 μm. These data suggest that outer and inner fiber diameter is well correlated (see Fig. 9).

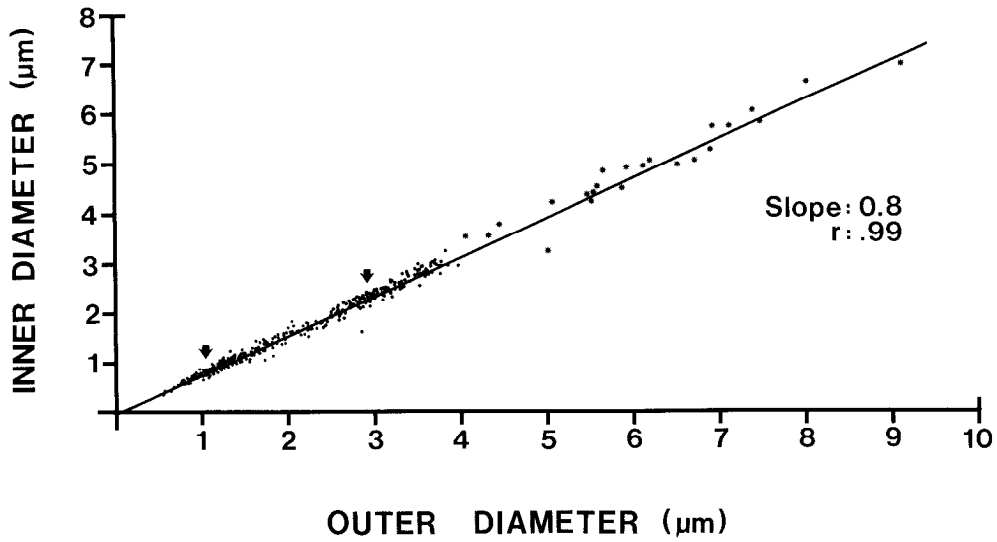

Figure 9. Plot of outer (x axis) versus inner (y axis) axon diameter. The sample of 471 fibers was taken from the right-central sector of AC1. The line of best fit correlates well ($r = 0.995$), has a slope of 0.8, and intersects the y axis at 0.06 μm. Seven fibers cut at, or close to, nodes of Ranvier were excluded from the data analysis. Two clusters of points, corresponding to small and intermediate size fibers, can be distinguished. *Arrows* point to the centers of these clusters. A dispersed group of 23 fibers have outer fiber diameters from 4.0 to 9.2 μm.

The central region of the cat retina contains a large number of comparatively small ganglion cells (Stone, 1965) which give rise to fine caliber axons (Stone and Holländer, 1971). This suggests that the high density crescent of the optic nerve contains a disproportionate number of axons originating within approximately 2 mm of area centralis. Alternatively, the fine fibers in the lateral crescent may contribute the uncrossed projection to lamina C1 of the lateral geniculate nucleus (Guillery, 1970) and to the superior colliculus. Thus, the peripheral crescent may contain a large number of W-type fibers originating from the temporal portion of the horizontal streak. According to Polyak (1957; see Figs. 201 and 202) topography is preserved along the entire course of the mammalian optic nerve. Although the recent observations of Horton et al. (1979) suggest that retinotopy within the optic nerve is quite coarse, this does not invalidate the foregoing interpretation. Insight into the significance of the peripheral crescent could be gained by tracing fibers of known origin with regard to the gradient in fiber density.

The relation between retinal ganglion cell type (X, Y, and W) and conduction velocity has been examined in considerable detail (Fukuda, 1971; Stone and Hoffmann, 1972; Cleland and Levick, 1974a, b; Stone and Fukuda, 1974; Rowe and Stone, 1976). The conduction velocity of W cells varies 5-fold—from 2.2 to 18 m/sec. Our data reveal a complementary 5-fold range in the caliber of the group of smaller axons: the very finest axons have diameters of 0.3 μm, whereas the largest of this small axon complement, as shown in the regional histograms, have diameters of 1.8 μm. The range of X cell conduction velocities is considerably less—at most from 9 to 23 m/sec (Rowe and Stone, 1976). The corresponding range of intermediate size axons in the regional analysis (e.g., Fig. 4) is 1.5 to 3.8 μm. Finally, the range of Y cell propagation velocity is from 20 to 40 m/sec, and this is reflected by a 2-fold range in the caliber of the largest group of axons—3.6 to 8.0 μm. Thus, there is an excellent correlation between the conduction velocity ranges of the three principal classes of retinal ganglion cells and the spectrum of fiber diameters. In contrast, Freeman (1978) has reported that conduction velocity of fibers in the cat's optic nerve correlates with myelin sheath thickness but, surprisingly, not with axon diameter. He further noted five discrete modes in the distribution of myelin sheath width in one adult cat which, nonetheless, had a unimodal fiber diameter spectrum. We can confirm neither of these results. Our data display a high correlation between the thickness of the myelin sheath and the axon diameter. In this respect our findings are in agreement with those of Friede et al. (1971) and Moore et al. (1976).

The bimodal distribution of axon diameter we have demonstrated contrasts with the *cumulative* unimodal distribution reported in previous investigations of the cat's optic nerve (G. H. Bishop and Clare, 1955; G. H. Bishop et al., 1969; van Crevel and Verhaart, 1963; Donovan, 1967; Fried et al., 1971; Hughes and Wässle, 1976; Freeman, 1978). However, two early studies have provided preliminary observations of a bimodal (P. O. Bishop et al., 1953) and even trimodal (Chang, 1952) distribution. In addition, Hughes and Wässle (1976) reported an ill-defined second mode in the peripheral population of optic axons. It must be emphasized that the present study provides the first evidence for a cumulative bimodal distribution of axon size within the optic nerve of any species of mammal.

A unimodal distribution of fiber caliber has been reported for the optic nerve of several other mammals, including monkey (Ogden and Miller, 1966; Potts et al., 1972), rat (Forrester and Peters, 1967; Hughes, 1977; Fukuda et al., 1982), brush-tailed possum and opposum (Freeman and Watson, 1978; Hokoç and Oswaldo-Cruz, 1978; Kirby et al., 1982), hamster (Rhoades et al., 1979), rabbit (Vaney and Hughes, 1976), and dolphin (Dawson et al., 1982). In view of our findings it may be appropriate to reassess fiber caliber spectra in species other than the cat. Preliminary work indicates that in the rhesus macaque optic nerve the cumulative fiber diameter spectrum is strictly unimodal (L. M. Chalupa and R. W. Williams, unpublished data).

Some studies of the cat nerve (G. H. Bishop and Clare, 1955; van Crevel and Verhaart, 1963; Donovan, 1967) employed light microscopy to determine axon caliber, and in these instances the failure to obtain a bimodal spectrum could be due to an inability to discern the finest fibers. However, it is less obvious why previous electron microscopic studies of the cat's optic nerve did not resolve a cumulative bimodal distribution. We believe two major methodological differences between the present study and those of others may account for this discrepancy. These involve the manner in which axon caliber is measured and the resolution with which the resulting data are plotted. First, in earlier studies axon caliber has been determined (*i*) by measuring the shortest distance bisecting the fiber (G. M. Bishop et al., 1969; Stone and Holländer, 1971), (*ii*) by taking the mean of the shortest and longest lines bisecting the axon (Freeman, 1978), or (*iii*) by the circle of best fit technique (Donovan, 1967; Hughes and Wässle, 1976). The latter method consists of obtaining the diameter of a circle which is estimated by eye to approximate the fiber cross-sectional area. The cross-sectional profiles of axons are by no means circular in the cat optic nerve (e.g., Fig. 2); therefore, the uniform application of such measurement criteria can be problematic. We believe that none of these methods provides an estimate of fiber size as accurate or as consistent as that obtained with the procedures employed in the present study. Second, the difference between the modes of the fiber spectrum is not much greater than 1 μm; therefore, the resolution employed to plot the fiber diameter data must be quite high. Our histograms of axon diameter have a bin width of 0.06 μm, whereas in prior studies bin widths have typically ranged from about 0.25 to 0.5 μm (e.g., Donovan, 1967; Hughes and Wässle, 1976; Freeman, 1978). In one early study (van Crevel and Verhaart, 1963) the frequency distribution for fiber caliber was plotted with a 2.0-μm bin width!

The demonstration of two distinct modes provides a sensitive method with which to assess the effects of experimental manipulations. For instance, it has recently been established that there are substantially more axons within the optic nerve of prenatal cats than in adult animals (Ng and Stone, 1982; Williams et al., 1983; R.

W. Williams, M. J. Bastiani, and L. M. Chalupa, manuscript in preparation). Furthermore, removal of one eye more than 2 weeks before birth results in a significant increase in the number of fibers within the remaining optic nerve (Williams et al., 1983). It would be of interest to examine the distribution of fiber caliber, both in nerve and tract, of animals enucleated before birth to determine whether the increment in fiber population is particular to one axon class.

References

Bishop, G. H., and M. H. Clare (1955) Organization and distribution of fibers in the optic tract of the cat. J. Comp. Neurol. *103:* 269–304.

Bishop, G. H., M. H. Clare, and W. M. Landau (1969) Further analysis of fiber groups in the optic tract of the cat. Exp. Neurol. *24:* 386–399.

Bishop, P. O., D. Jeremy, and J. W. Lance (1953) The optic nerve. Properties of a central tract. J. Physiol. (Lond.) *121:* 415–432.

Boycott, B. B., and H. Wässle (1974) The morphological types of ganglion cells of the domestic cat's retina. J. Physiol. (Lond.) *240:* 397–419.

Chang, H. -T. (1952) Functional organization of central visual pathways. Res. Publ. Assoc. Res. Nerv. Ment. Dis. *30:* 430–453.

Chang, H. -T. (1965) Fiber groups in the primary optic pathway of the cat. J. Neurophysiol. *19:* 224–231.

Cleland, B. G., and W. R. Levick (1974a) Brisk and sluggish concentrically organized ganglion cells in the cat's retina. J. Physiol. (Lond.) *240:* 421–456.

Cleland, B. G., and W. R. Levick (1974b) Properties of rarely encountered types of ganglion cells in the cat's retina and an overall classification. J. Physiol. (Lond.) *240:* 457–492.

Cleland, B. G., M. W. Dubin, and W. R. Levick (1971) Sustained and transient neurones in the cat's retina and lateral geniculate nucleus. J. Physiol. (Lond.) *217:* 473–496.

Cleland, B. G., W. R. Levick, and K. J. Sanderson (1973) Properties of sustained and transient ganglion cells in the cat retina. J. Physiol. (Lond.) *228:* 649–680.

Cullheim, S., and B. Ulfhake (1979) Relations between cell body size, axon diameter and axon conduction velocity of triceps surae alpha motoneurons during the postnatal development in the cat. J. Comp. Neurol. *188:* 679–686.

Dawson, W. W., M. N. Hawthorne, R. L. Jenkins, and R. T. Goldston (1982) Giant neural systems in the inner retina and optic nerve of small whales. J. Comp. Neurol. *205:* 1–7.

Donovan, A. (1967) The nerve fibre composition of the cat optic nerve. J. Anat. *101:* 1–11.

Enroth-Cugell, C., and J. G. Robson (1966) The contrast sensitivity of retinal ganglion cells of the cat. J. Physiol. (Lond.) *187:* 517–552.

Forrester, J., and A. Peters (1967) Nerve fibres in optic nerve of rat. Nature (Lond.) *214:* 245–247.

Freeman, B. (1978) Myelin sheath thickness and conduction latency groups in the cat optic nerve. J. Comp. Neurol. *181:* 183–196.

Freeman, B., and C. R. R. Watson (1978) The optic nerve of the brush-tailed possum, *Trichosurus vulpecula*: Fibre diameter spectrum and conduction latency groups. J. Comp. Neurol. *179:* 739–752.

Friede, R. L., T. Miyaghishi, and K. Hao Hu (1971) Axon calibre, neurofilaments, microtubules, sheath thickness and cholesterol in cat optic nerve fibres. J. Anat. *108:* 365–373.

Fukuda, Y. (1971) Receptive field organization of cat optic nerve fibres with special reference to conduction velocity. Vision Res. *11:* 209–226.

Fukuda, Y., T. Sugimoto, and T. Shirokawa (1982) Strain differences in quantitative analysis of the rat optic nerve. Exp. Neurol. *75:* 525–532.

Gasser, H. S., and H. Grundfest (1939) Axon diameters in relation to the spike dimensions and the conduction velocity in mammalian A fibers. Am. J. Physiol. *127:* 393–414.

Goldman, L., and J. S. Albus (1968) Computation of impulse conduction in myelinated fibres: Theoretical basis of the velocity-diameter relation. Biophys. J. *8:* 596–607.

Guillery, R. W. (1970) The laminar distribution of retinal fibers in the dorsal lateral geniculate nucleus of the cat: A new interpretation. J. Comp. Neurol. *138:* 339–368.

Guillery, R. W., E. H. Polley, and F. Torrealba (1982) The arrangement of axons according to fiber diameter in the optic tract of the cat. J. Neurosci. 714–721.

Hoffmann, K. -P. (1973) Conduction velocity in pathways from retina to superior colliculus in the cat: A correlation with receptive-field properties. J. Neurophysiol. *36:* 409–421.

Hokoç, J. N., and E. Oswaldo-Cruz (1978) Quantitative analysis of the opossum's optic nerve: An electron microscope study. J. Comp. Neurol. *178:* 773–782.

Horton, J. C., M. M. Greenwood, and D. H. Hubel (1979) Non-retinotopic arrangement of fibres in cat optic nerve. Nature (Lond.) *282:* 720–722.

Hughes, A. (1977) The pigmented rat optic nerve: Fibre count and fibre diameter spectrum. J. Comp. Neurol. *176:* 263–268.

Hughes, A., and H. Wässle (1976) The cat optic nerve: Fiber total count and diameter spectrum. J. Comp. Neurol. *169:* 172–184.

Illing, R. -B., and H. Wässle (1981) The retinal projection to the thalamus in the cat: A quantitative investigation and a comparison with the retinotectal pathway. J. Comp. Neurol. *202:* 265–285.

Jack, J. J. B., D. Noble, and R. W. Tsien (1975) *Electric Current Flow in Excitable Cells*, Clarendon Press, Oxford.

Kelly, J. P., and C. D. Gilbert (1975) The projections of different morphological types of ganglion cells in the cat retina. J. Comp. Neurol. *163:* 65–80.

Kirby, M. A., L. Clift-Forsberg, P. D. Wilson, and S. C. Rapisardi (1982) Quantitative analysis of the optic nerve of the North American opossum (*Didelphis Virginiana*): An electron microscopic study. J. Comp. Neurol. *212:* 318–327.

Kornguth, S. E., P. D. Spear, and E. Langer (1982) Reduction in number of large ganglion cells in cat retina following intravitreous injection of antibodies. Brain Res. *245:* 35–45.

Lennie, P. (1980) Parallel visual pathways: A review. Vision Res. *20:* 561–594.

Leventhal, A. G., J. Keens, and I. Tork (1980) The afferent ganglion cells and cortical projections of the retinal recipient zone of the cat's pulvinar complex. J. Comp. Neurol. *194:* 535–554.

Magalhães-Castro, H. H., L. A. Murata, and B. Magalhães-Castro (1976) Cat retinal ganglion cells projecting to the superior colliculus as shown by the horseradish peroxidase method. Exp. Brain Res. *25:* 541–549.

Moore, C. L., R. Kalil, and W. Richards (1976) Development of myelination in optic tract of the cat. J. Comp. Neurol. *125:* 125–136.

Ng, A. Y. K., and J. Stone (1983) The optic nerve of the cat: Appearance and loss of axons during normal development. Dev. Brain Res. *5:* 263–271.

Ogden, T. E., and R. F. Miller (1966) Studies of the optic nerve of the rhesus monkey: Nerve fiber spectrum and physiological properties. Vision Res. 485–506.

Peichl, L., and H. Wässle (1979) Size, scatter and coverage of ganglion cell receptive field centres in the cat retina. J. Physiol. (Lond.) *291:* 117–141.

Polyak, S. (1957) *The Vertebrate Visual System.* University of

Chicago Press, Chicago.

Potts, A. M., D. Hodges, S. B. Shelman, K. J. Fritz, N. S. Levy, and Y. Mangnall (1972) Morphology of the primate optic nerve. II. Total fiber size distribution and fiber density distribution. Invest. Ophthalmol. *11:* 989–1003.

Rhoades, R. W., L. Hsu, and G. Parfett (1979) An electron microscopic analysis of the optic nerve in the golden hamster. J. Comp. Neurol. *186:* 491–504.

Rodieck, R. W. (1973) *The Vertebrate Retina*, Freeman, San Francisco.

Rowe, M. J., and J. Stone (1976) Conduction velocity groupings among axons of cat retinal ganglion cells, and their relationship to retinal topography. Exp. Brain Res. *25:* 339–357.

Rushton, W. A. H. (1951) A theory of the effects of fibre size in medullated nerve. J. Physiol. (Lond.) *115:* 101–122.

Spear, P. D., K. R. Jones, S. R. Zetlan, E. E. Geisert, and S. E. Kornguth (1982) Effects of antibodies to large ganglion cells on the cat's retinogeniculate pathway. J. Neurophysiol. *47:* 1174–1195.

Stone, J. (1965) A quantitative analysis of the distribution of ganglion cells in the cat's retina. J. Comp. Neurol. *124:* 337–352.

Stone, J., and J. E. Champion (1978) Estimate of the number of myelinated axons in the cat's optic nerve. J. Comp. Neurol. *180:* 799–806.

Stone, J., and R. Clarke (1980) Correlation between soma size and dendtritic morphology in cat retinal ganglion cells: Evidence of further variation in the γ-cell class. J. Comp. Neurol. *192:* 211–217.

Stone, J., and Y. Fukuda (1974) Properties of cat retinal ganglion cells. A comparison of W-cells with X- and Y-cells. J. Neurophysiol. *37:* 722–748.

Stone, J., and K. -P. Hoffmann (1972) Very slow-conducting ganglion cells in the cat's retina: A major, new functional type? Brain Res. *43:* 610–616.

Stone, J., and H. Holländer (1971) Optic nerve axon diameter measured in the cat retina: Some functional considerations. Exp. Brain Res. *13:* 498–503.

van Crevel, H., and W. J. C. Verhaart (1963) The rate of secondary degeneration in the central nervous system. II. The optic nerve of the cat. J. Anat. *97:* 451–464.

Vaney, D. I., and A. Hughes (1976) The rabbit optic nerve: Fibre diameter spectrum, fibre count, and comparison with a retinal ganglion cell count. J. Comp. Neurol. *170:* 241–252.

Wässle, H., and R. -B. Illing (1980) The retinal projection to the superior colliculus in the cat: A quantitative study with HRP. J. Comp. Neurol. *190:* 333–356.

Wässle, H., B. B. Boycott, and R. -B. Illing (1981) Morphology and mosaic of on- and off-beta cells in the cat retina and some functional considerations. Proc. R. Soc. Lond. Biol. *212:* 177–195.

Waxman, S. G., and H. A. Swadlow (1977) The conduction velocity of axons in central white matter. Prog. Neurobiol. *8:* 297–324.

Williams. R. W., M. J. Bastiani, and L. M. Chalupa (1983) Loss of axons in the cat optic nerve following fetal unilateral enucleation: An electron microscopic analysis. J. Neurosci. *3:* 133–144.